

Finite element analysis of rectangular waveguide with deformation as depression and protrusion of side walls

A S Chaudhari and P B Patil*

Department of Physics, Dr. B A M University, Aurangabad-431 004,
Maharashtra, India

Received 7 February 1996, accepted 19 August 1996

Abstract : X-band rectangular waveguide with depression and protrusion on the vertical size is analysed using Finite Element Method by keeping the corner points fixed. Five cases of waveguide deformed, depression on one side, depression on both sides, protrusion on one side, protrusion on both sides, depression on one side and protrusion on other side, are considered. For each case, the effect on TE₁₀, TE₂₀ mode and passband is worked out. The variation in TE₁₀, TE₂₀ mode and bandwidth is observed for each case.

Keywords : Finite element analysis, rectangular waveguide, depression and protrusion

PACS Nos. : 02.70.Dh, 84.40.Az

1. Introduction

The waveguide with arbitrary shape is analysed by Bulley and Davies [1] using Rayleigh Ritz method. Single and double V groove waveguides are analysed by Li *et al* [2] using combination of transverse resonance method and numerical integration technique.

In this paper, we have analysed the rectangular waveguide with depression and protrusion on vertical size using Finite Element Method for five cases (Figure 1) :

- case (1) Depression on one side,
- case (2) Depression on both side,
- case (3) Protrusion on one side,
- case (4) Protrusion on both side,
- case (5) Depression on one side and protrusion on other side.

* Author for correspondence.

For each case, for different L in the step of 0.15 cm, the eigenvalues and eigenvectors are obtained. The TE₁₀ and TE₂₀ mode are identified using field plotting. The variation

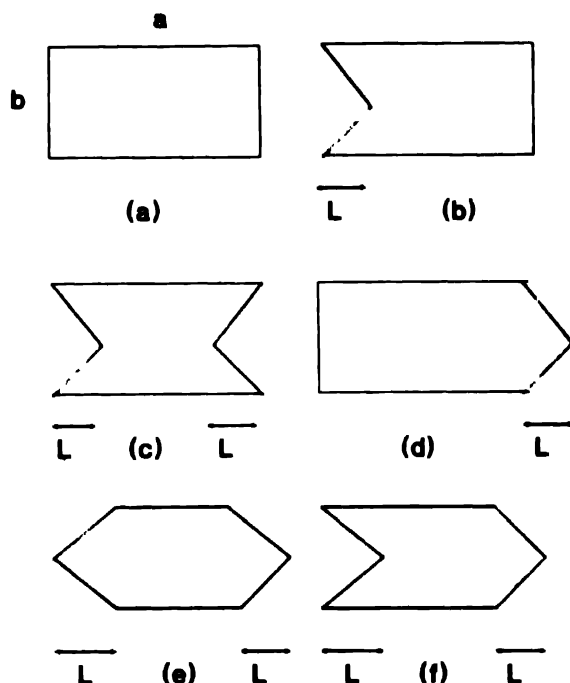


Figure 1. (a) Rectangular wave guide. (b) Rectangular wave guide with depression on one vertical side. (c) Rectangular wave guide with depression on both vertical sides. (d) Rectangular wave guide with protrusion on one vertical side. (e) Rectangular wave guide with protrusion on both vertical sides. (f) Rectangular waveguide with depression on one vertical side and protrusion on other vertical side.

of frequencies for TE₁₀ and TE₂₀ mode and bandwidth with L is represented graphically.

2. Statement of the problem

Consider a homogeneous rectangular waveguide, with perfect conducting walls (Figure 1), enclosing air as a dielectric medium.

The electric and magnetic fields inside the waveguide, will satisfy the Maxwell's equations and assuming the time dependance of the fields as $\exp(j\omega t)$, the Maxwell's equation are written as

$$\nabla \times \mathbf{E} = -j\omega\mu_0\mathbf{H}, \quad (1)$$

$$\nabla \times \mathbf{H} = -j\omega\epsilon_0\epsilon\mathbf{E}. \quad (2)$$

To avoid the spurious solution [3], the magnetic field vector formulation is used for the solution of the problem. Therefore Maxwell's eq. (2) is expressed as

$$\epsilon^{-1}(\nabla \times \mathbf{H}) = j\omega\epsilon_0\mathbf{E}. \quad (3)$$

Taking the curl of eq. (3) and using eq. (1), eq. (3) can be written as

$$\nabla \times (\epsilon^{-1}\nabla \times \mathbf{H}) = K_0^2 \mathbf{H}, \quad (4)$$

where $K_0^2 = \omega^2\mu_0\epsilon_0$.

Here ω is the angular frequency, ϵ_0 and μ_0 are the permittivity and permeability of free space and ϵ is the relative permittivity of the medium, inside the waveguide. Since there is air medium inside the waveguide, so $\epsilon = 1$.

The magnetic field \mathbf{H} must satisfy the suitable boundary condition at the conducting boundaries it being that the normal component of the magnetic field is zero on conductor boundaries.

$$\mathbf{H} \cdot \mathbf{n} \Big|_{\text{boundary}} = 0. \quad (5)$$

Thus the problem of electromagnetic propagation under consideration, involves solving of eq. (4) subjected to condition eq. (5).

3. Variational formulation

To get the expression for the functional Π , the eq. (4) is multiplied by a arbitrary test function \mathbf{V}^* and then integrated over the domain of the problem. This leads to an expression for functional as

$$\Pi = \int_{\Omega} \mathbf{V}^* \cdot \nabla \times (\epsilon^{-1}\nabla \times \mathbf{H}) d\Omega - \int_{\Omega} \mathbf{V}^* \cdot K_0^2 \mathbf{H} d\Omega. \quad (6)$$

Using vector identity for the first term in eq. (6) and converting volume integral into surface integral, we get eq. (6) as

$$\begin{aligned} \Pi = \int_{\Gamma} \mathbf{n} \cdot (\epsilon^{-1}\nabla \times \mathbf{H} \times \mathbf{V}) d\Gamma + \int_{\Omega} (\epsilon^{-1}\nabla \times \mathbf{H}) \cdot (\nabla \times \mathbf{V}^*) d\Omega \\ - \int_{\Omega} \mathbf{V}^* \cdot K_0^2 \mathbf{H} d\Omega, \end{aligned} \quad (7)$$

$$\begin{aligned} \Pi = \int_{\Gamma} \mathbf{V}^* \cdot [\mathbf{n} \times (\epsilon^{-1}\nabla \times \mathbf{H})] d\Gamma + \int_{\Omega} (\epsilon^{-1}\nabla \times \mathbf{H}) \cdot (\nabla \times \mathbf{H}^*) d\Omega \\ - \int_{\Omega} \mathbf{V}^* \cdot K_0^2 \mathbf{H} d\Omega. \end{aligned} \quad (8)$$

Since tangential component of \mathbf{E} is continuous at the boundary. The first term in eq. (8) will be zero i.e. $\mathbf{n} \cdot (\epsilon^{-1} \nabla \times \mathbf{H}) = 0$. Using Galerkin criteria as $\mathbf{V}^* = \mathbf{H}^*$ (complex conjugate of \mathbf{H}), the functional Π will become bilinear and symmetric. The bilinear terms are multiplied by 1/2 and we get functional

$$\Pi = \frac{1}{2} \int_{\Omega} [(\nabla \times \mathbf{H}^*) \cdot (\epsilon^{-1} \nabla \times \mathbf{H}) - K_0^2 \mathbf{H}^* \cdot \mathbf{H}] d\Omega. \quad (9)$$

4. Finite element formulation

According to standard finite element method [4,5], the domain of (cross section of waveguide) the problem is divided into number of rectangular elements and the functional is transferred over each element.

Let Π^e represents functional over the element. Then

$$\begin{aligned} \Pi^e = \sum_{ele} [& \left(\int_{\Omega^e} (\nabla \times \mathbf{H}^{e*}) \cdot (\epsilon^{-1} \nabla \times \mathbf{H}^e) d\Omega^e \right. \\ & \left. - \int_{\Omega^e} K_0^2 \mathbf{H}^{e*} \cdot \mathbf{H}^e d\Omega^e \right)], \end{aligned} \quad (10)$$

where the unknown \mathbf{H}^e is a vector which has three components H_x , H_y and H_z . Each unknown component H_x , H_y , H_z is defined in terms of the nodal values H^e_x , H^e_y , H^e_z respectively.

For a typical element contribution, introduce the linear mapping function $\{\psi^e\}$ such that

$$\{H\} = \{\psi^e\}^T \{H^e\} = \{H^e\}^T \{\psi^e\}, \quad (11)$$

where $\{H^e\}^T = \{H^1_x, H^1_y, H^1_z, H^2_x, H^2_y, H^2_z,$

$$H^3_x, H^3_y, H^3_z, H^4_x, H^4_y, H^4_z\} \quad (12)$$

and $\{\psi^e\}^T = \begin{Bmatrix} \psi_1 & 0 & 0 & \psi_2 & 0 & 0 & \psi_3 & 0 & 0 & \psi_4 & 0 & 0 \\ 0 & \psi_1 & 0 & 0 & \psi_2 & 0 & 0 & \psi_3 & 0 & 0 & \psi_4 & 0 \\ 0 & 0 & i\psi_1 & 0 & 0 & i\psi_2 & 0 & 0 & i\psi_3 & 0 & 0 & i\psi_4 \end{Bmatrix}. \quad (13)$

$$\nabla \times \mathbf{H} = \begin{bmatrix} 0 & -\frac{\partial}{\partial z} & \frac{\partial}{\partial y} \\ \frac{\partial}{\partial z} & 0 & -\frac{\partial}{\partial x} \\ \frac{\partial}{\partial y} & \frac{\partial}{\partial x} & 0 \end{bmatrix} \begin{bmatrix} H_x \\ H_y \\ H_z \end{bmatrix}$$

$$\nabla \times \mathbf{H} = [A]_{3 \times 3} \{\psi^e\}_{3 \times 12}^T \{H^e\}_{12 \times 1} = \{B^e\}_{3 \times 12}^T \{H^e\}_{12 \times 1}$$

$$[A] = \begin{bmatrix} 0 & -\frac{\partial}{\partial z} & \frac{\partial}{\partial y} \\ \frac{\partial}{\partial z} & 0 & -\frac{\partial}{\partial x} \\ \frac{\partial}{\partial y} & \frac{\partial}{\partial x} & 0 \end{bmatrix}$$

So $\nabla \times \mathbf{H} = \{B^e\}^T \{H^e\} = \{H^e\}^T \{B^e\},$ (14)

where $\{B^e\}^T = [A] \{\psi^e\}^T$ and $\{B^e\} = [A]^T \{\psi^e\}.$ (15)

Substitution of eq. (11) and (15) in eq. (10) gives

$$\begin{aligned} \Pi^e = & \frac{1}{2} \sum_{\text{elm}} \left[\int_{\Omega^e} \{H^e\}^T \{B^e\}^* \epsilon^{-1} \{B^e\}^T \{H^e\} d\Omega^e \right. \\ & \left. - \int K_0^2 \{H^e\}^T \{\psi^e\}^* \{\psi^e\}^T \{H^e\} d\Omega^e \right]. \end{aligned} \quad (16)$$

Taking $\{H^e\}^T$; as a common multiplier and $\{H^e\}$ as common post multiplier we get,

$$\begin{aligned} \Pi^e = & \sum_{\text{elm}} \{H^e\}^T \frac{1}{2} \left[\int_{\Omega^e} \{B^e\}^* \epsilon^{-1} \{B^e\}^T d\Omega^e \right. \\ & \left. - \int_{\Omega^e} K_0^2 \{\psi^e\}^* \{\psi^e\}^T d\Omega^e \right] \{H^e\}, \\ \Pi^e = & \sum_{\text{elm}} \frac{1}{2} \{H^e\}^T [S^e] \{H^e\} - \frac{1}{2} K_0^2 \sum_{\text{elm}} \{H^e\}^T [T^e] \{H^e\}, \end{aligned} \quad (17)$$

where $[S^e] = \int_{\Omega^e} \{B^e\}^* \epsilon^{-1} \{B^e\}^T d\Omega^e,$ (18)

$$[T^e] = \int_{\Omega^e} \{\psi^e\}^* \{\psi^e\}^T d\Omega^e. \quad (19)$$

The functional for the whole region Ω is given by

$$\Pi = \frac{1}{2} \{H\}^T [S] \{H\} - \frac{1}{2} K_0^2 \{H\}^T [T] \{H\}. \quad (20)$$

Variation of eq. (20) w.r.t. the nodal variation, leads to the following eigenvalue problem.

$$[S] \{H\} - K_0^2 [T] \{H\} = 0. \quad (21)$$

Eq. (21) is the matrix equation to be solved for eigen values $K_0^2 = \lambda.$

5. Divergence condition

The formulation in eq. (20) gives the number of spurious solutions. These spurious solutions do not satisfy the relation $\nabla \cdot \mathbf{H} = 0$. Therefore, this divergence term is included in the variational formulation.

6. Numerical calculations

For first case, the depression L from one side is increased in the step of 0.15 cm. For second case, the depression L from both sides is increased in the step of 0.15 cm in opposite

Table 1. f in GHz for TE10 and TE20 mode with depression in the step of 0.15 cm on one side

Sr. no.	Depression cm	f in GHz		Bandwidth in GHz
		TE10	TE20	
1	0.1500	6.4795	13.0123	6.5328
2	0.3000	6.7599	13.5418	6.7818
3	0.4500	7.1192	14.1941	7.0749
4	0.6000	7.5727	14.9810	7.4084
5	0.7500	8.1307	15.8891	7.7584
6	0.9000	8.8055	16.8825	8.0770
7	1.0500	9.6135	17.9052	8.2917
8	1.2000	10.5742	18.9899	8.3247
9	1.3500	11.7037	19.8460	8.1423

Table 2. f in GHz for TE10 and TE20 mode with depression in the step of 0.15 cm on both sides

Sr. no.	Depression cm	f in GHz		Bandwidth in GHz
		TE10	TE20	
1	0.1500	6.7151	13.4718	6.7567
2	0.3000	7.3402	14.6205	7.2803
3	0.4500	8.2209	16.0790	7.8581
4	0.6000	9.4722	17.7705	8.2983
5	0.7500	11.2277	19.4369	8.2092
6	0.9000	13.4793	21.0385	7.5591
7	1.0500	15.4468	22.9447	7.4978

Table 3. f in GHz for TE₁₀ and TE₂₀ mode with protrusion in the step of 0.15 cm on one side

Sr. no.	Depression cm	f in GHz		Bandwidth in GHz
		TE ₁₀	TE ₂₀	
1	0.1500	6.0861	12.2240	6.1379
2	0.3000	5.9582	11.9501	5.9919
3	0.4500	5.8750	11.7617	5.8867
4	0.6000	5.8294	11.6489	5.8195
5	0.7500	5.8110	11.5926	5.7816
6	0.9000	5.8110	11.5751	5.7641
7	1.0500	5.8235	11.5845	5.7609
8	1.2000	5.8450	11.6130	5.7679
9	1.3500	5.8734	11.6557	5.7823

Table 4. f in GHz for TE₁₀ and TE₂₀ mode with protrusion in the step of 0.15 cm on both sides.

Sr. no.	Depression cm	f in GHz		Bandwidth in GHz
		TE ₁₀	TE ₂₀	
1	0.1500	5.9223	11.8883	5.9660
2	0.3000	5.6845	11.3816	5.6971
3	0.4500	5.5342	11.0455	5.5113
4	0.6000	5.4522	10.8468	5.3946
5	0.7500	5.4170	10.7432	5.3262
6	0.9000	5.4117	10.7006	5.2889
7	1.0500	5.4260	10.6972	5.2712
8	1.2000	5.4539	10.7199	5.2660
9	1.3500	5.4914	10.7603	5.2689

Table 5. f in GHz for TE10 and TE20 mode with depression on one side and protrusion on the other side in the step of 0.15 cm.

Sr. no.	Depression cm	f in GHz		Bandwidth in GHz
		TE10	TE20	
1	0.1500	6.2947	12.6351	6.3405
2	0.3000	6.4129	12.8267	6.4138
3	0.4500	6.6350	13.1932	6.5581
4	0.6000	6.9738	13.7487	6.7749
5	0.7500	7.4335	14.4785	7.0450
6	0.9000	8.0199	15.3527	7.3328
7	1.0500	8.7434	16.3263	7.5829
8	1.2000	9.6130	17.3366	7.7236
9	1.3500	10.6325	18.3190	7.6865

direction. For third case, the protrusion L on one side is increased in the step of 0.15 cm. For fourth case, the protrusion L in the step of 0.15 cm in opposite direction is increased.

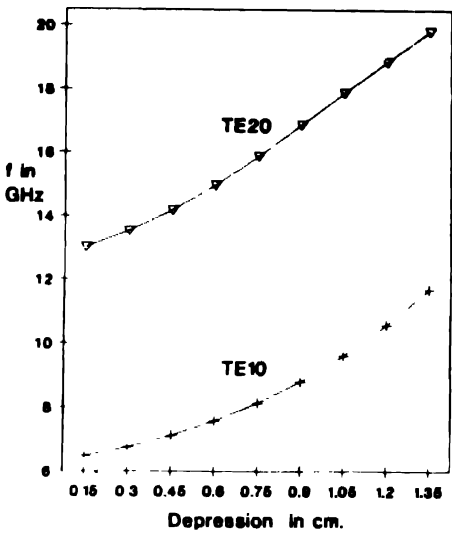


Figure 2. Variation of f for TE10 and TE20 with depression L on one vertical side.

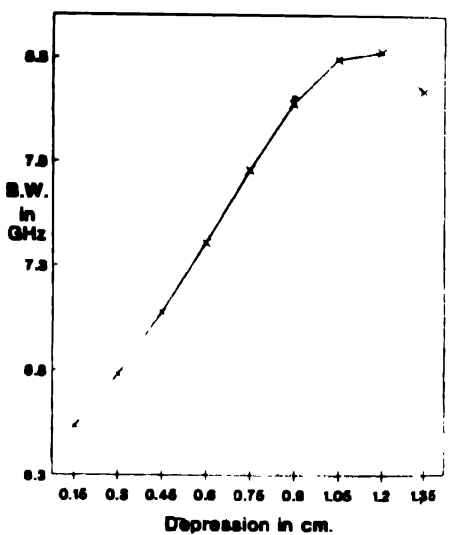


Figure 3. Variation of bandwidth with depression L on one vertical side.

Finally, in the fifth case, the protrusion L from one side and depression L on another in the step of 0.15 cm is considered.

For each L , the eigenvalues and eigenvectors are worked out by running the FEM programme [6–8]. The obtained eigenvalues are the values of $\omega^2\mu_0\epsilon_0$. Using these eigenvalues, corresponding frequencies f are calculated. These frequencies are compared with the X-band rectangular waveguide which are 6.2590 GHz for TE₁₀ mode, 12.5788 GHz for TE₂₀ mode and the bandwidth is 6.3197 GHz. For each case, for each L , the values of f in GHz are given in Tables 1 to 5. The variation of f and bandwidth with L , for each case, are shown graphically in Figures 2 to 11.

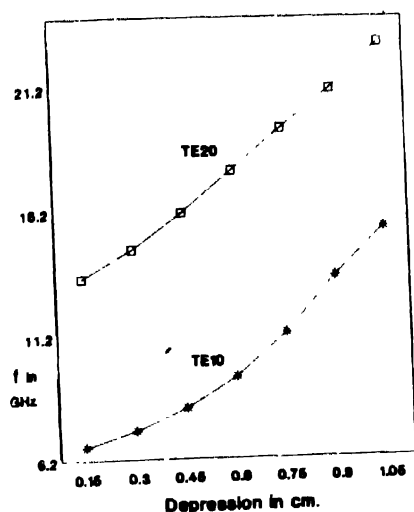


Figure 4. Variation of f for TE₁₀ and TE₂₀ with depression L on both vertical sides.

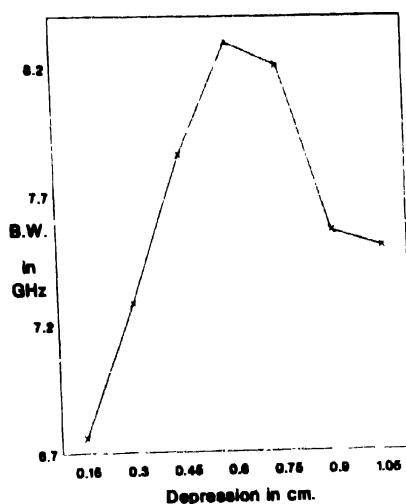


Figure 5. Variation of bandwidth with depression L on both vertical sides.

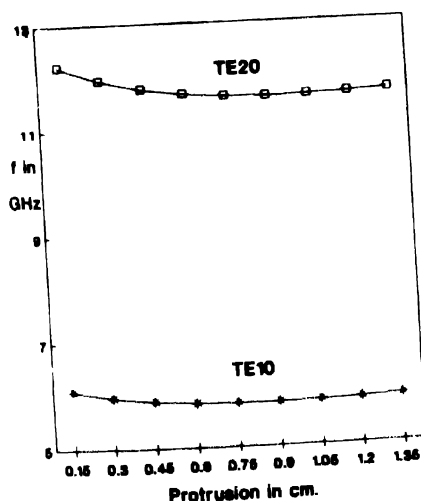


Figure 6. Variation of f for TE₁₀ and TE₂₀ with protrusion L on one vertical side.

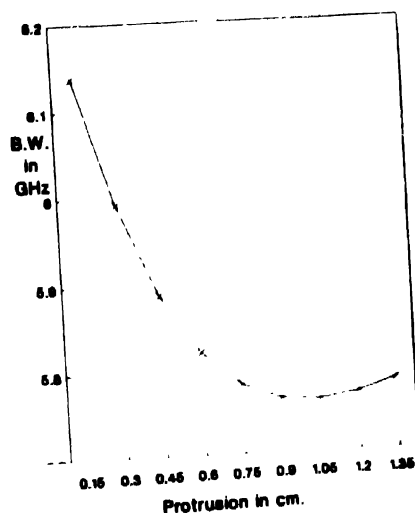


Figure 7. Variation of bandwidth with protrusion L on one vertical side.

7. Conclusion

For depression on one or both vertical sides of the waveguide, the frequencies for TE₁₀ and TE₂₀ mode increase and the bandwidth also increases. On the other hand, for the protrusion on one or both vertical side of the waveguide, the TE₁₀ and TE₂₀ mode frequencies first decrease and then increase slightly whereas the bandwidth decreases.

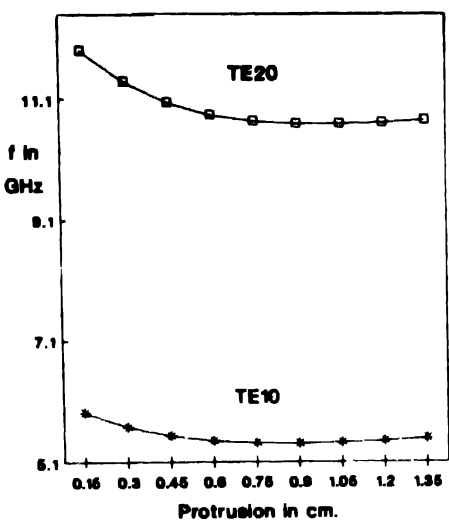


Figure 8. Variation of f for TE₁₀ and TE₂₀ with protrusion L on both vertical sides.

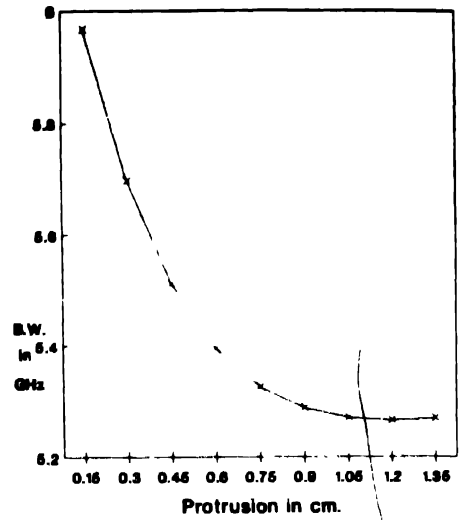


Figure 9. Variation of bandwidth with protrusion L on both vertical sides.

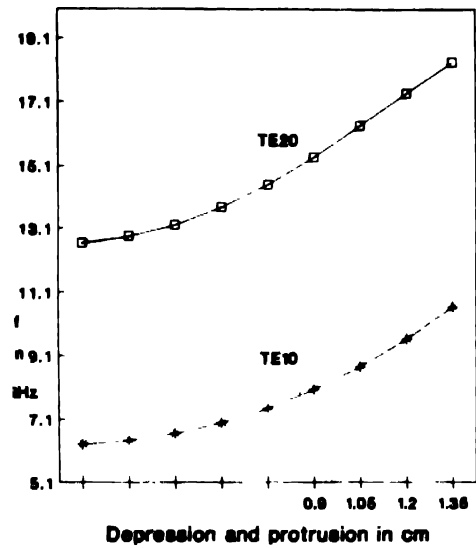


Figure 10. Variation of f for TE₁₀ and TE₂₀ with depression on one vertical side and protrusion on other vertical side.

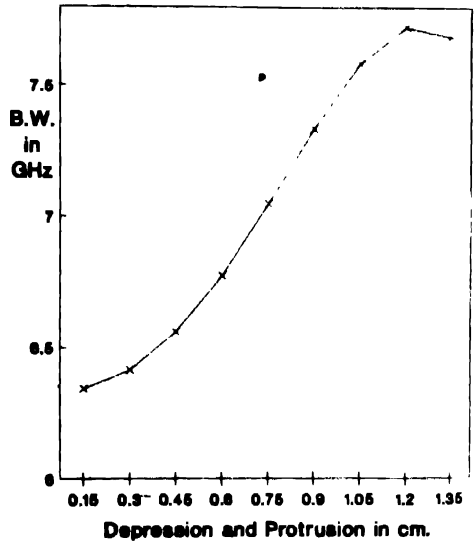


Figure 11. Variation of bandwidth with depression on one vertical side and protrusion on other vertical side.

For the combination of depression and protrusion, the results are same as for the depression, only the values of the frequencies and bandwidth are higher.

The above conclusions lead us to the concept that the X-band rectangular slotline can be used for KU band also, merely by inserting two metallic wedges near its vertical sides.

References

- [1] R M Bulley and J B Davies *IEEE Trans. Microwave Theory and Techniques* vol MTT-17 p 440 (Aug. 1969)
- [2] Si Fan Li, Zhong Xiang Shen and Xiao Ming Lou *IEEE Trans. On Microwave Theory and Technique* Vol. 39 No.8 p 1413 (August 1991)
- [3] K Hayata, M Koshiba, M Eguchi and M Suzuki *IEEE Trans. Microwave Theory and Technique* Vol MTT-34 p 1120 (Nov. 1986)
- [4] J N Reddy *An Introduction to Finite Element Method* (New York: Mc-Graw-Hill) (1991)
- [5] J E Akin *Application and Implementation of Finite Element Method* (New York: Academic) (1988)
- [6] G M Kalmase and P B Patil *Indian J. Pure Appl. Phys.* **32** 899 (1994)
- [7] Manasi Karkare, A S Chaudhari and P B Patil *Indian J. Phys.* **70B** 487 (1996)
- [8] S K Popalghat *PhD Thesis* (Submitted to Dr. B. A. M. University, Aurangabad, India) (1995)